INTERNATIONAL JOURNAL FOR NUMERICAL METHODS IN FLUIDS
Int. J. Numer. Meth. Fluids 2006; **51**:1017–1039
Published online 15 March 2006 in Wiley InterScience (www.interscience.wiley.com). DOI: 10.1002/fld.1205

An Eulerian approach to fluid–structure interaction and goal-oriented mesh adaptation

Th. Dunne*,†

Institute of Applied Mathematics, University of Heidelberg, Germany

SUMMARY

We propose an Eulerian framework for modelling fluid–structure interaction (FSI) of incompressible fluids and elastic structures. The model is based on an Eulerian approach for describing structural dynamics. This is achieved by tracking the movement of the initial positions of all 'material' points. In this approach the displacement appears as a primary variable in an Eulerian framework.

Our approach uses a technique which is similar to the level set method in so far that it also tracks initial data, in our case the set of initial positions (IP), and from this determines to which 'phase' a point belongs. To avoid the occasional reinitialization of the initial position set we employ the harmonic continuation of the structure velocity field into the fluid domain.

By using the IP set for tracking the structure displacement, we can ensure that corners and edges of the fluid–structure interface are preserved well.

Based on this monolythic model of the FSI we apply the *Dual Weighted Residual* (DWR) method for goal-oriented *a posteriori* error estimation to stationary FSI problems.

Examples are presented based on the model and for the goal-oriented local mesh adaptation.

KEY WORDS: Eulerian model for fluid–structure interaction; initial position method; level set method; *a posteriori* error estimator; goal-oriented mesh adaptation

1. INTRODUCTION

Two large domains of numerical simulation of physical systems are computational fluid dynamics and computational structure dynamics. With the introduction of high performance computing, attention has started to shift to systems consisting of a coupling of fluid and structure dynamics.

*Correspondence to: Th. Dunne, Institute of Applied Mathematics, University of Heidelberg, INF 294/293, 69120 Heidelberg, Germany.
†E-mail: thomas.dunne@iwr.uni-heidelberg.de

Contract/grant sponsor: German Research Foundation (DFG); contract/grant number: FG 493
Contract/grant sponsor: University of Heidelberg

Received 2 June 2005
Revised 8 December 2005
Accepted 18 January 2006

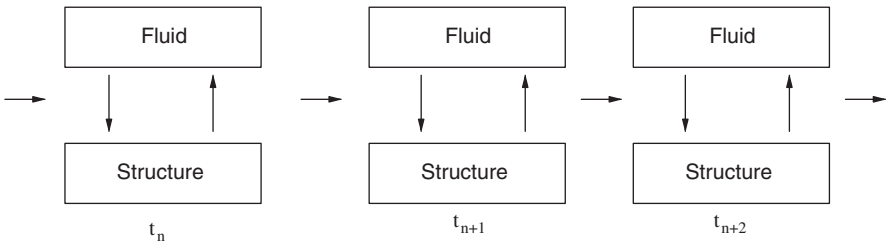

Figure 1. Partitioned approach, Lagrangian and Eulerian frameworks coupled.

General examples of fluid–structure interaction entail flow containing elastic particles (particulate flow), flow around elastic structures (airplanes, submarines) and flow in elastic structures (haemodynamics, transport of fluids in closed containers). In all these settings the immediate dilemma though when confronted with the task of modelling the coupled dynamics is that the fluid model is conventionally based on an Eulerian perspective in contrast to the conventional Lagrangian approach for the solid model.

Combining these two perspectives in one common description can be troublesome. On the one hand, the fluid domain itself is time-dependent and depends on the deformation of the structure domain. On the other hand, for the structure the fluid boundary values (velocity and the normal component of the stress tensor) are needed. In both cases values from the one problem are used (optionally interpolated) for the other, this is costly and can lead to a loss of accuracy.

A known approach is to separate the two models, solve each separately, and so converge iteratively to a solution which satisfies both (Figure 1). Solving the separated problems serially multiple times is referred to as a partitioned approach; each system is solved conventionally, and one iterates between the systems until the interface conditions are satisfied. A partitioned approach does not permit for the problem to be written in a complete variational formulation. To do this usually an auxiliary unknown domain transformation function T is introduced for the fluid domain. With this the fluid problem is rewritten as one on the transformed domain[‡] (Figure 2). For this see arbitrary Lagrangian–Eulerian (ALE) methods [1–3] and deforming space–time finite element formulations [4, 5]. Both the partitioned and the transformation approach to the Euler–Lagrange discrepancy explicitly track the mesh and are generally referred to as interface tracking methods. For both of them the structure problem is left in the Lagrangian framework.

As a third possibility we propose rewriting the structure problem in an Eulerian framework. A similar approach has been demonstrated by Liu and Walkington [6]. Once rewritten in a complete Eulerian framework, a phase variable is employed on the fixed mesh to differentiate between the different phases. This approach to identifying the interface is generally referred to as interface capturing, a method commonly used for simulating multiphase flows [7, 8].

[‡]We show in Figure 2 *merely as an example to this approach* the domains and reference domains of a driven cavity problem as described in the second example in Section 6. Calculations would be done on the reference domains. As a part of calculations the auxiliary transformation function T has to be determined at each timestep.

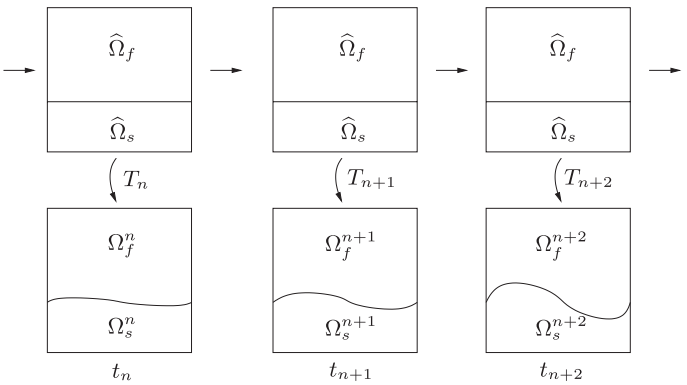

Figure 2. Transformation approach, both frameworks Lagrangian.

Examples for the use of a phase variable are the volume of fluid method (VOF) [9] and the level set method [10–12].

With the level set approach the distance function has to continually be reinitialized, due to the convection velocity in the fluid domain. The two traits (signed distance function and reinitialization) make modelling FSI problems with cornered structures difficult using a level set approach.

The approach we use is a variation to the level set method that makes reinitialization unnecessary and for which cornered structures pose less of a problem.

The method we describe does not necessitate any specific structure model. The key variable in structure dynamics is the displacement gradient, and since this depends on the displacement, it is understandable why it is preferably described in the Lagrangian perspective.

To be able to provide the displacements in an Eulerian sense we introduce the *set of initial positions* (IP set) of all structure points. These are then transported with the structure velocity at each time step. Based on the IP set and their Eulerian coordinates the displacements are now available in an Eulerian sense. (The displacement gradient has to be rewritten appropriately in an Eulerian approach, this we explain later in Section 3.2.) Since the fluid–structure interface will be crossing through cells we will have to also transport the IP set in the fluid domain.

If we were to use the fluid velocity for the convection of the IP set this would lead to entanglement of the respective displacements, which would 'wreak havoc' on the interface cells. This is a known problem with level set approaches. A common method of fixing this problem has been to occasionally fix the level set field between the time steps. The problem with this method is that the variational formulation is no longer consistent.

As an alternative we harmonically continue the structure velocity into the fluid domain. In the fluid domain we then use this velocity for the convection of the IP set. Since an IP set is available in both domains, we can always at each point determine if it belongs to the fluid or solid part of the model.

Again this approach is similar to the level set approach [10]. It is possible using the level set approach to also develop a model for FSI [13]. But when developing a complete variational formulation, especially if the interface contains corners, the two key characteristics of the

level set approach also become the main cause of concern: reinitialization and the signed distance function. Although the problem of reinitialization here can also be avoided by using an harmonically continued velocity, the trouble concerning corner approximation stays.

In contrast to this, by using an initial position set we are deforming a virtual grid of the structure extended into the whole domain. Based on this grid, corners on the structure boundaries are approximated better.

The equations we use are based on the momentum and mass conservation equations for the flow of an incompressible Newtonian fluid and the deformation of an incompressible neo-Hookean solid.

The outline of this paper is as follows; in Section 2 we introduce the necessary notations. In Section 3 the approach and consequently combined equations are presented. In Section 4 the discrete finite element formulations are presented. To insure robustness of systems the Local Projection Stabilization scheme is used [14]. In Section 5 results for an example are shown. In Section 6 for a stationary case we present an *a posteriori* error estimator, which is based on the solution of the dual variational problem [15–17]. This we use for goal-oriented local mesh adaptation.

2. NOTATION

All behaviour takes place in the polygonal domain $\Omega \subset \mathbb{R}^d$ (d being 2 or 3). Later for the discretization we use a finite element mesh $\mathbb{T}_h$ of Ω for the the finite element method. The cells of the mesh $\mathbb{T}_h$ we denote with K.

This domain contains the two time-dependent subdomains: the fluid domain $\Omega_f(t)$ and the structure domain $\Omega_s(t)$. We will, unless needed, forgo writing the time-dependency of these domains.

The boundaries of Ω, Ω_f, Ω_s we denote, respectively, as $\partial\Omega$, $\partial\Omega_f$, $\partial\Omega_s$. The common interface between Ω_f and Ω_s we denote as $\Gamma_i(t)$ or simply Γ_i.

The initial structure domain we denote as $\widehat{\Omega}_s$. Similarly spaces, domains, coordinates, values (such as pressure, displacement, velocity) and operators based on $\widehat{\Omega}_s$ (or $\widehat{\Omega}_f$) will have an additional hat.

With $L^2(X)$ we denote the Lebesque space of square-integrable functions on X equipped with the inner product and norm

$$(f,g)_X := \int_X fg \,\mathrm{d}x, \quad \|f\|_X^2 = (f,f)_X$$

For tensor valued functions F and G we denote the tensor product

$$(F:G)_X = \int_X \sum_{i,j} F_{ij}G_{ij}$$

Generally the domain X will be Ω, in which case we will forgo supplying the domain index with all products and norms. For Ω_f, Ω_s we similarly denote the respective spaces, products and norms with a respective index of 'f' or 's'. All $L^2(X)$ functions (with $X = \Omega$, $\Omega_f(t)$, $\Omega_s(t)$) with generalized (in the weak sense) first-order derivatives in $L^2(X)$ we assign to the Sobolev space $H^1(X)$. Appropriately we denote $H_0^1(X) = \{v \in H^1(X) : v_{|\partial X} = 0\}$.

Two frequently used function spaces will be L_X and V_X

$$L_X := L^2[0,T;L^2(X)^d], \quad V_X := H^1[0,T;L^2(X)^d] \cap L^2[0,T;H_0^1(X)^d]$$

Again, the X-index will be omitted in the case of Ω and for Ω_f, Ω_s a respective index of 'f' or 's' will be used.

Partial derivatives of f to the ith component we denote with $\partial_i f$. The total time-derivative of f we denote with $d_t f$. The divergences of vectors and tensors we note as $\operatorname{div} f = \sum_i \partial_i f_i$ and $(\operatorname{div} F)_i = \sum_j \partial_j F_{ij}$. The gradient of a vector valued function v we denote as a tensor, $(\nabla v)_{ij} = \partial_j v_i$.

With $[f]$ we denote the jump of a function value on a common element edge or an inner boundary. With the value n we mean the unit vector n at each point of that boundary. For example $[\sigma \cdot n]$ on the edge of an an element $K \in \mathbb{T}_h$ denotes the jump of $\sigma \cdot n$ across the boundary of K to the respective neighbouring element K' with normal unit vector n at each point of that boundary. If K has no respective neighbouring element at a certain part of its boundary then we define the 'jump' value there as $[\sigma \cdot n] = 2\sigma \cdot n$.

3. FORMULATION

3.1. Fluid

For the liquid we observe a Newtonian incompressible fluid governed by the equations based on the conservation of mass and momentum. The equations are set in an Eulerian framework in the time-dependent domain $\Omega_f(t)$. For this we use the scalar pressure field $p_f \in L_f$ and the vector velocity field $v_f \in v_{fD} + V_f$. Here v_{fD} is a suitable extension of the prescribed Dirichlet data on the respective boundaries (both moving and stationary) of Ω_f and g_1 is a suitable extension to all of $\partial\Omega_f$ of the Neumann values of $\sigma_f \cdot n$ prescribed on the respective boundaries. We have 'hidden' the fluid–structure interface conditions of steadiness of velocity and normal stress in parts of the boundary conditions v_{fD} and g_1. These are addressed below in Section 3.3. We write the equations in the variational form.

Find $\{v_f, p_f\} \in \{v_{fD} + V_f\} \times L_f$, so that

$$\begin{aligned} (\rho_f \partial_t v_f + \rho_f (v_f \cdot \nabla) v_f, \psi_v)_f + (\sigma_f : \varepsilon(\psi_v))_f &= (g_1, \psi_v)_{\partial\Omega_s} + (f_1, \psi_v)_s \quad && \forall \psi_v \in V_f \\ (\operatorname{div} v_f, \psi_p)_f &= 0 && \forall \psi_p \in L_f \end{aligned} \tag{1}$$

with $\sigma_f := -p_f I + 2\rho_f \nu_f \varepsilon(v_f)$, $\varepsilon(x) := \frac{1}{2}(\nabla x + \nabla x^{\mathrm{T}})$.

3.2. Structure

For the structure we observe a neo-Hookean incompressible elastic medium also governed by the equations based on the conservation of mass and momentum. Usually the equations are set in a Lagrangian framework in the domain $\widehat{\Omega}_s$ with the scalar pressure field $\widehat{p}_s \in \widehat{L}_f$ and the vector displacement and velocity fields $\widehat{u}_s \in \widehat{u}_D + \widehat{V}_s$, $\widehat{v}_s \in \widehat{v}_D + \widehat{V}_s$. Here $\widehat{u}_D$ and $\widehat{v}_{sD}$ are suitable extensions of the prescribed Dirichlet data on the respective boundaries of $\widehat{\Omega}_s$ and $\widehat{g}_2$ is a suitable extension to all of $\partial\widehat{\Omega}_s$ of the Neumann values of $\widehat{\sigma}_s \cdot n$ prescribed on the respective boundaries. Again, similar to the fluid problem, we have 'hidden' the fluid–structure interface

conditions of steadiness of velocity and normal stress in parts of the boundary conditions $\widehat{v}_{sD}$ and $\widehat{g}_2$. These are addressed below in Section 3.3. We assume for the sake of simplicity that the only boundary displacements that take place are on $\widehat{\Gamma}_i$: $\widehat{u}_D = \widehat{v}_{sD} = 0\ \forall x \in \partial\widehat{\Omega}_s \backslash \widehat{\Gamma}_i$. We write the equations in the variational form.

Find $\{\widehat{u}_s,\ \widehat{v}_s,\ \widehat{p}_s\} \in \{\widehat{u}_D + \widehat{V}_s\} \times \{\widehat{v}_{sD} + \widehat{V}_s\} \times \widehat{L}_s$, so that

$$
\begin{aligned}
(\rho_s d_t \widehat{v}_s, \widehat{\psi})_{\widehat{s}} + (\widehat{\sigma}_s \widehat{F}^{-\mathrm{T}} : \widehat{\varepsilon}(\widehat{\psi}))_{\widehat{s}} &= (\widehat{g}_2, \widehat{\psi})_{\partial\widehat{\Omega}_s} + (\widehat{f}_2, \widehat{\psi})_{\widehat{s}} \quad && \forall \widehat{\psi} \in \widehat{V}_s \\
(d_t \widehat{u}_s - \widehat{v}_s, \widehat{\psi})_{\widehat{s}} &= 0 && \forall \widehat{\psi} \in \widehat{V}_s \\
(\det \widehat{F}, \widehat{\psi})_{\widehat{s}} &= (1, \widehat{\psi})_{\widehat{s}} && \forall \widehat{\psi} \in \widehat{L}_s
\end{aligned}
$$

with $\widehat{F} := I + \widehat{\nabla}\widehat{u}_s$, $\widehat{\sigma}_s := -\widehat{p}_s I + \mu_s(\widehat{F}\widehat{F}^{\mathrm{T}} - 1)$, $\widehat{\varepsilon}(x) := \frac{1}{2}(\widehat{\nabla}x + \widehat{\nabla}x^{\mathrm{T}})$.

To write these conservation equations in an Eulerian perspective we will need the pressure $\widehat{p}_s$, displacement $\widehat{u}_s$ and displacement gradient $\widehat{\nabla}\widehat{u}_s$ available in an Eulerian sense: p_s, u_s, ∇u_s.

Since we will be solving in the Eulerian formulation, values that are not operator based can simply be rewritten: $p_s(x) = \widehat{p}_s(\widehat{x})$, $u_s(x) = \widehat{u}_s(\widehat{x})$. Formally this means

$$
\begin{aligned}
p_s(x) &= \widehat{p}_s(D(x)) = \widehat{p}_s(\widehat{x}) \\
u_s(x) &= \widehat{u}_s(D(x)) = \widehat{u}_s(\widehat{x})
\end{aligned}
\tag{2}
$$

Here $D(x)$ is the deformation function of points in the deformed domain Ω_s to points in the initial domain $\widehat{\Omega}_s$. The analogous inverse deformation function is $\widehat{D}(\widehat{x})$

$$
\begin{aligned}
\widehat{D} &: \widehat{\Omega}_s \to \Omega_s, \widehat{D}(\widehat{x}) = \widehat{x} + \widehat{u}_s = x \\
D &: \Omega_s \to \widehat{\Omega}_s, D(x) = x - u_s = \widehat{x}
\end{aligned}
\tag{3}
$$

Since $\det \widehat{\nabla}\widehat{D} = \det \widehat{F} = 1$ the deformations D, $\widehat{D}$ are well defined.

The immediate difficulty with Equation (2) is that u_s is determined by $\widehat{u}_s$ and, by way of $D(x)$, itself. This is unpractical, since $u(x)$ cannot be determined directly. As an usable alternative, we need a direct way of determining the displacement $u(x)$ that a 'material' point at x has gone through regarding its initial position at point $\widehat{x}$.

To achieve this we introduce the *set of initial positions* of all points: $\phi \in V$. If we look at a given 'material' point at the position $x \in \Omega$ and the time $t \in (0, T]$, then the value $\phi(t,x)$ will tell us what the initial position of this point was at $t = 0$. These points are transported in the full domain with a certain velocity $w \in V$. The convection velocity in the structure will be the structure velocity itself $w_{|\Omega_s} = v_s$. If the fluid velocity were to be used for convection in the fluid domain, then the displacements there would eventually become very entangled. For this reason we use an alternative velocity. This we explain later below in Section 3.3. We write the equations in the variational form.

Find $\phi \in \phi_0 + V$, so that

$$
(\partial_t \phi, \psi) + ((w \cdot \nabla)\phi, \psi) = 0 \quad \forall \psi \in V \tag{4}
$$

Here ϕ_0 is a suitable extension of the prescribed Dirichlet data on the respective boundaries

$$
\begin{aligned}
\phi(0,x) &= x \quad \forall x \in \Omega \\
\phi(t,x) &= x \quad \forall \{t,x\} \in (0,T] \times \partial\Omega
\end{aligned}
$$

For any point with the initial position $\hat{x}$ and later at time t the position x this means

$$\hat{x} + \hat{u}(t,\hat{x}) = x$$

Since $\hat{x} = \phi(0,\hat{x}) = \phi(t,x)$ and $\hat{u}(t,\hat{x}) = u(t,x)$ it follows:

$$x = \phi + u \tag{5}$$

Applied to the IP set Equation (4)

$$(-\partial_t u, \psi) + (w - (w\cdot\nabla)u, \psi) = 0 \quad \forall \psi \in V$$

To access the Eulerian displacement gradient we use an identity of the deformation functions from (3): $D(\hat{D}(\hat{x})) = \hat{x}$. Deriving this with chain rule leads to

$$(I - \nabla u)(I + \hat{\nabla}\hat{u}) = I \;\Leftrightarrow\; \hat{\nabla}\hat{u} = (I - \nabla u)^{-1} - I$$

Thus the Cauchy stress tensor σ_s can be specified for a neo-Hookean incompressible material in an Eulerian framework

$$\sigma_s = -p_s I + \mu_s(FF^{\mathrm{T}} - 1)$$
$$F = I + \hat{\nabla}\hat{u} = (1 - \nabla u)^{-1}$$

Finally we write the structure equations in the Eulerian framework in the time-dependent domain $\Omega_s(t)$ with the respective scalar pressure field p_s, the vector displacement and velocity fields u_s, v_s. The usual incompressibility condition $\det(F) = 1$ we replace with the equation for divergence conservation of the velocity.

Find $\{u_s, v_s, p_s\} \in \{u_D + V_s\} \times \{v_{sD} + V_s\} \times L_s$, so that

$$\begin{aligned}
(\rho_s \partial_t v_s + \rho_s(v_s\cdot\nabla)v_s, \psi)_s + (\sigma_s : \varepsilon(\psi))_s &= (g_2, \psi)_{\partial\Omega_s} + (f_2, \psi)_s \quad && \forall \psi \in V_s \\
(\partial_t u_s, \psi)_s + (-v_s + (v_s\cdot\nabla)u_s, \psi)_s &= 0 && \forall \psi \in L_s \\
(\operatorname{div} v_s, \psi)_s &= 0 && \forall \psi \in L_s
\end{aligned} \tag{6}$$

with $F := (1 - \nabla u)^{-1}$, $\sigma_s := -p_s I + \mu_s(FF^{\mathrm{T}} - 1)$.

3.3. Combined equations

Since both the the fluid and structure equations (1), (6) for conservation of mass and momentum are now in an Eulerian framework, they can be combined into one unified formulation. Included in the Neumann condition is the condition that the normal stress of the fluid $\sigma_f\cdot n$ should be equal to the normal stress of the structure $\sigma_s\cdot n$. By using one common field for the velocity the steadiness of velocity on Γ_i becomes implied. Any possible Dirichlet velocity conditions of v_{fD} and v_{sD} that were on $\partial\Omega$ we combine to a suitable velocity field $v_D \in V$. The Neumann conditions $\sigma_f\cdot n = \sigma_s\cdot n$ that are present at the common interface Γ_i now appear as a boundary integral of the jump $[\sigma\cdot n]$ on the right-hand side

$$([\sigma\cdot n], \psi_v)_{\Gamma_i} = \int_{\Gamma_i} (\sigma_f - \sigma_s)\cdot n_f \psi_v \, \mathrm{d}x$$

By omitting this boundary integral from the right-hand side the steadiness of $\sigma\cdot n$ becomes an implicit condition of the combined variational formulation. The left over parts of g_1, g_2 are

now just the Neumann boundary conditions on $\partial\Omega$. These we combine to g_3. We write the Cauchy stress tensor for the whole domain

$$\sigma := \chi_f \sigma_f + \chi_s \sigma_s$$

Here χ_f, χ_s are the characteristic functions of Ω_f, Ω_s which are determined by the values of the IP set ϕ

$$\chi_f(t,x) = \begin{cases} 1, & \phi(t,x) \in \widehat{\Omega}_f \backslash \widehat{\Gamma}_i \\ 0, & \phi(t,x) \in \widehat{\Omega}_s \end{cases} \tag{7}$$

$$\chi_s = 1 - \chi_f$$

The interface Γ_i will (usually) be intersecting mesh cells. Due to this we will need a reasonable continuation of the displacement and the displacement gradient from the structure domain into the fluid domain. The value of u in the fluid domain will be determined by the choice of the convection velocity w. If we were to use the fluid velocity this would eventually lead to ever increasing entanglement, which would necessitate a continual reinitialization of the IP set. As an alternative we use the harmonic continuation of the structure velocity.

Find $\phi \in \phi_0 + V$, so that

$$\begin{aligned} (\partial_t \phi, \psi) + ((w \cdot \nabla)\phi, \psi) &= 0 \quad \forall \psi \in V \\ (\chi_s (w - v), \psi) &= 0 \quad \forall \psi \in V \\ (\chi_f \nabla w, \nabla \psi) &= 0 \quad \forall \psi \in V \end{aligned} \tag{8}$$

We combine the formulations (1), (6), (8) and (7) with (5).

Find $\{v, w, u, p\} \in \{v_D + V\} \times V \times V \times L$, so that

$$\begin{aligned} (\rho \partial_t v + \rho (v \cdot \nabla) v, \psi) + (\sigma : \psi) &= (g_3, \psi)_{\partial\Omega} + (f_3, \psi) \quad \forall \psi \in V \\ (\operatorname{div} v, \psi) &= 0 \quad \forall \psi \in L \\ (\partial_t u - w + (w \cdot \nabla) u, \psi) &= 0 \quad \forall \psi \in L \\ (\chi_s (w - v), \psi) + (\chi_f \nabla w, \nabla \psi) &= 0 \quad \forall \psi \in V \end{aligned}$$

with

$$\begin{aligned} \rho &:= \chi_f \rho_f + \chi_s \rho_s \\ \sigma &:= \chi_f \sigma_f + \chi_s \sigma_s \\ \sigma_f &:= -pI + 2\rho_f \nu_f \varepsilon(v), \quad \sigma_s := -pI + \mu_s (FF^{\mathrm{T}} - I) \\ F &:= (I - \nabla u)^{-1} \\ \chi_f &:= \begin{cases} 1, & x - u \in \widehat{\Omega}_f \backslash \widehat{\Gamma}_i \\ 0, & x - u \in \widehat{\Omega}_s \end{cases} \\ \chi_s &= 1 - \chi_f \end{aligned} \tag{9}$$

4. FINITE ELEMENT DISCRETIZATION

4.1. Mesh notations

For the discretization a conforming finite element Galerkin method is used on meshes $\mathbb{T}_h$ consisting of quadrilateral (or hexaedral in 3d) elements. The cells of the meshes we denote with K. The mesh parameter h is a scalar cellwise constant field that as a value is assigned the diameter of the cell on each cell. Refinement of a cell consists of dividing a cell into four subcells by drawing 'vertical' and 'horizontal' lines through the midpoints of the edges. Coarsening of four cells is possible if these four cells were obtained by refinement of a larger cell and none of the four cells have hanging nodes on their edges. The *finest level* of cells on a mesh $\mathbb{T}_h$ consists of all cells that can be removed by coarsening in one sweep. The coarsened mesh is referred to as $\mathbb{T}_{2h}$. To facilitate mesh refinement we allow a cell to have a node that is on the midpoint of the edge of a neighbouring cell. These *hanging nodes* cannot have any degrees of freedom and their values are the interpolations of the values on the points of the larger edge. For details to this approach see Reference [18].

4.2. Galerkin formulation

With the arguments $U = \{v, w, u, p\}$, $\Psi = \{\psi_v, \psi_w, \psi_u, \psi_p\} \in W := V \times V \times V \times L$ we write Equations (9) as a semilinear form

$$\begin{aligned} a(U, \Psi) := {} & (\rho \partial_t v + \rho(v \cdot \nabla)v, \psi_v) + (\sigma(U) : \varepsilon(\psi_v)) \\ & + (\operatorname{div} v, \psi_p) - (g_3, \psi_v)_{\partial\Omega} - (f_3, \psi_v) \\ & + (\partial_t u - w + (w \cdot \nabla)u, \psi_u) \\ & + (\chi_s(w - v), \psi_w) + (\chi_f \nabla w, \nabla \psi_w) \end{aligned}$$

With this we write the problem in a compact form

$$\text{Find } U \in U_0 + W, \text{ so that}$$
$$a(U, \Psi) = 0 \quad \forall \Psi \in W$$

Here U_0 is an extension of certain Dirichlet boundary conditions. As a discretization of the functions spaces we use one that is Q1 for all components, similar to the Q1/Q1 Stokes element. See References [19, 20].

The corresponding finite element subspaces we denote by $L_h \subset L$, $V_h \subset V$, $W_h \subset W$. As time-stepping methods we use the implicit Euler method in the first example and later in the second example the Fractional-Step θ scheme [21–24].

4.3. Local projection stabilization scheme

Since we use an 'equal-order interpolation' in our elements, they lack stability and the necessary discrete 'inf-sup stability' (or Babuska–Brezzi) condition for pressure and velocity (or displacement) is not satisfied. We circumvent this by using the 'Local Projection Stabilization' (LPS) scheme introduced by Becker and Braack as described in Reference [14].

Additionally we also use this method to stabilize the convection terms. We define the mesh- and parameter-dependent bilinear form

$$(\varphi,\psi)_\delta := \sum_{K\in\mathbb{T}_h} \delta_K\ (\varphi,\psi)_K$$

$$\delta_K = \alpha(\chi_f \rho_f v_f h_K^{-2} + \chi_s \mu_s h_K^{-2} + \beta\rho|v_h|_{\infty;K} h_K^{-1})^{-1}$$

With this we define $s_\delta(U_h,\Psi_h)$ as the sum of the following stabilization terms:

- pressure: $(\nabla\pi_h p_h, \nabla\pi_h\Psi_{p,h})_\delta$,
- transport: $(\rho v_h\cdot\nabla\pi_h v_h, v_h\cdot\nabla\pi_h\Psi_{v,h})_\delta$.

Here π_h is the 'fluctuation operator' on the finest level of the mesh $\mathbb{T}_h$. Based on the L^2-projection operator $P_{2h}: V_h \to V_{2h}$, it measures the fluctuation of a function in V_h in regards to its projection into the next coarse space V_{2h}

$$\pi_h : V_h \to V_{2h}, \quad \pi_h = I - P_{2h}$$

The stabilized Galerkin approximation of the problem can be written

Find $U_h \in U_{0,h} + W_h$ so that

$$a_\delta(U_h,\Psi_h) := a(U_h,\Psi_h) + s_\delta(U_h,\Psi_h) = 0 \quad \forall\Psi_h \in W_h$$

Two remarkable features are that the stabilization terms only act on the diagonal of the coupled system and that no second derivatives are needed. This stabilization is called weakly consistent since the introduced terms vanish for $h\to 0$. The values α, β for the stabilization parameter δ_K are chosen manually, our results are based on $\alpha = 1/2$, $\beta = 1/6$.

5. FIRST EXAMPLE

As a first example we simulate a configuration that is being used in the DFG research group FG 493. There are many teams in the DFG research group FG 493 and the simulation results all vary to some degree. One of the purposes of this group is the comparison of numerical methods and results based on standardized experimental setups. In this example the most recent intermediate results given by one of the groups calculate the final solution to be similar but not identical to our results. It is not clear if the differences in the results stem from using different numerical approaches or different code libraries. To ensure a useful comparison of results, we have also implemented an ALE-based approach using our numerics library Gascoigne [25]. As we explained in the introduction, this approach is based on the idea of transforming the time-dependent fluid domain back to its initial reference domain with an auxiliary functional T in each time-step. A good description of this approach is given by Hron in [1].

The example is based on the successful DFG 'flow around a cylinder' benchmark [26].

The domain dimensions are: length $L = 2.5$, height $H = 0.41$. The left bottom corner is at $(0,0)$. The circle centre is positioned at $C = (0.2, 0.2)$ with the radius $r = 0.05$. The elastic structure bar has the length $l = 0.35$ and height $h = 0.02$. Its right lower end is positioned at $(0.6, 0.19)$, the left end is fully attached to the cylinder. The flag material point A is initially

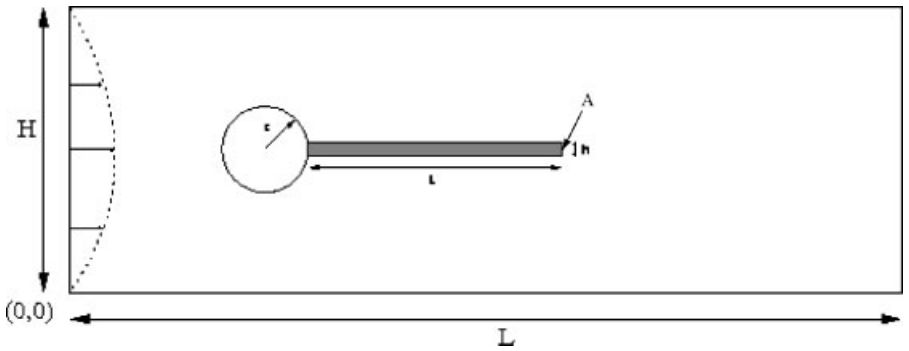

Figure 3. Diagram of first example.

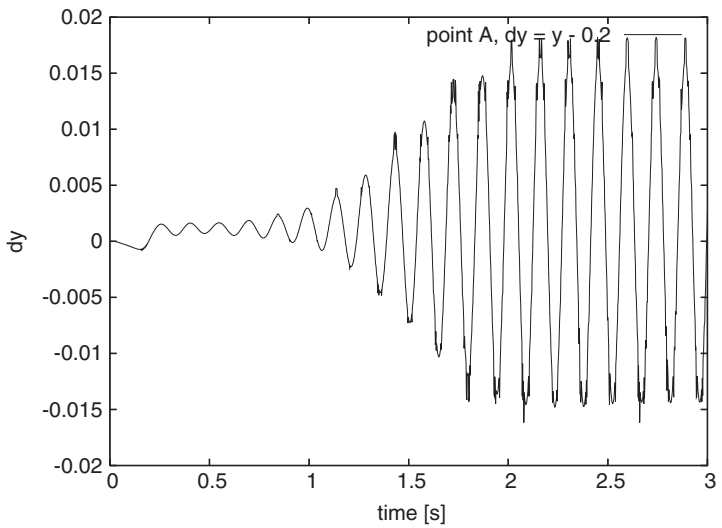

Figure 4. Vertical Displacement of the material point A: Eulerian approach.

positioned at $(0.6, 0.20)$. The point A is at the trailing tip of the structure; its position will change during the course of a simulation (Figure 3).

Boundary conditions: except for the in- and outflow boundaries, we choose the 'no-slip' condition. As an inflow condition we set a parabolic velocity profile on the left side of the channel: $v(0, y) = 3.0y(H - y)/(H/2)^2$. As an outflow condition we choose the 'stress free' Neumann condition: $\sigma \cdot n = 0$. As an initial condition the velocity is zero and there is no deformation of the structure. The right-hand side is set to zero. In this example the fluid and structure constants are: $\rho_f = \rho_s = 1.0\text{e}3$, $\nu_f = 1.0\text{e-}3$, $\mu_s = 2.0\text{e}6$. As a time-step size we use 0.005 s.

The results shown in the Figures 4 and 5 are the vertical displacements of the point A. For both approaches we obtain a periodic flag oscillation. For the Eulerian approach we obtain an

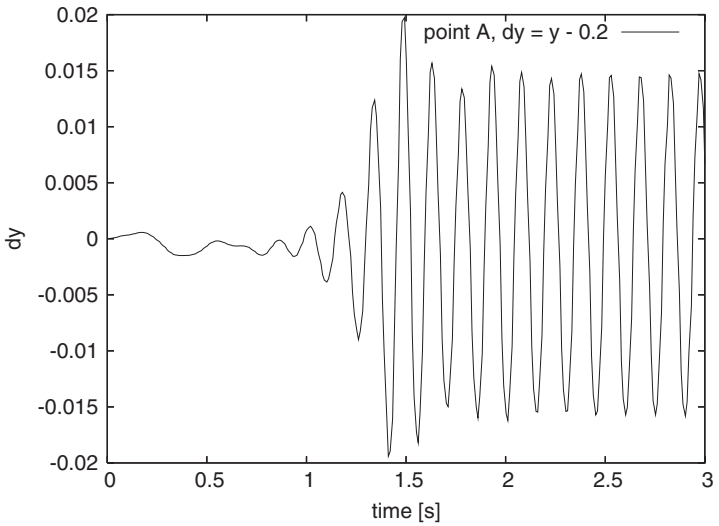

Figure 5. Vertical Displacement of the material point A: ALE approach.

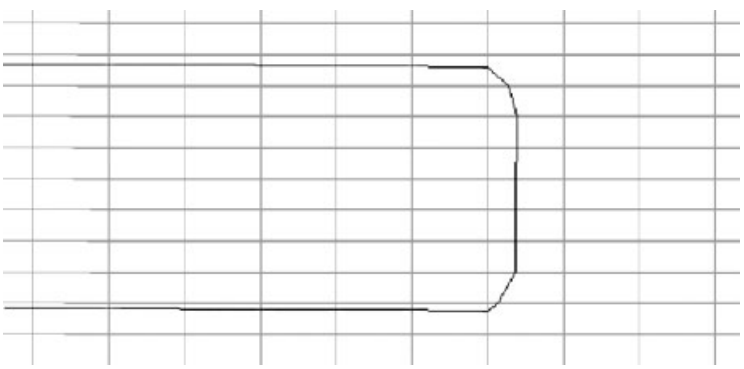

Figure 6. Approximation per level set.

amplitude of 1.6e-2 with a frequency of 6.86 s^{-1}. In comparison to that, based on the ALE approach, we obtain an amplitude of 1.51e-2 with a frequency of 6.70 s^{-1}. These results are in good agreement with each other, especially when considering how much the results can vary as experience in our research group has shown.

In the two figures below (Figures 6 and 7) we compare the interface approximations of the end of the flag from the simulation based on the use of a level set and an initial position set. In Figure 6 the interface is identified by all points for which $\phi = 0$. In Figure 7 the interface is identified by all points which are on one of the respective isoline segments belonging to the edges of the flag. The significant differences are visible in the cells that contain the corners. Since the structure deformations are not in a Lagrangian framework, it is not immediately clear, due to the coupling with the fluid, how well (or how bad) the mass of the structure is

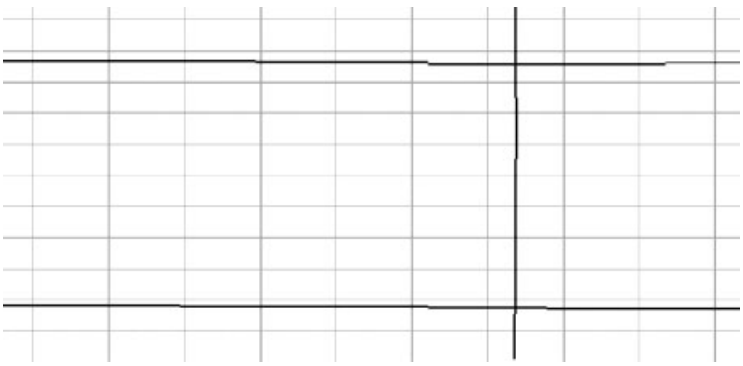

Figure 7. Approximation per initial position set.

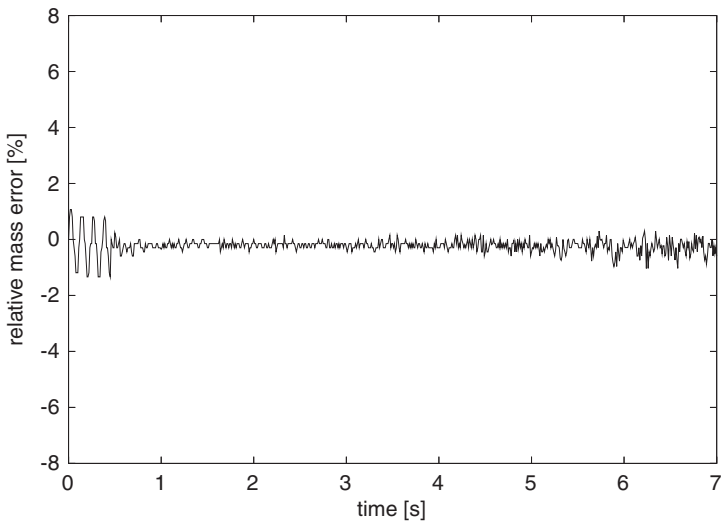

Figure 8. Relative mass error of the flag.

conserved in an Eulerian approach, especially during the course of an instationary simulation after hundreds of time steps. In Figure 8 we display the flag's relative mass error in the course of the simulation. Except for certain initial jitters, the relative error is less than 1%.

6. SECOND EXAMPLE

In the second example we apply the model to a modified driven cavity configuration. This is a driven cavity with an elastic volume at the bottom, which we configure so that a visible stationary solution can be expected (Figure 9). To this effect we make the material very soft and also remove convection from both systems. To this we apply the *Dual Weighted Residual*

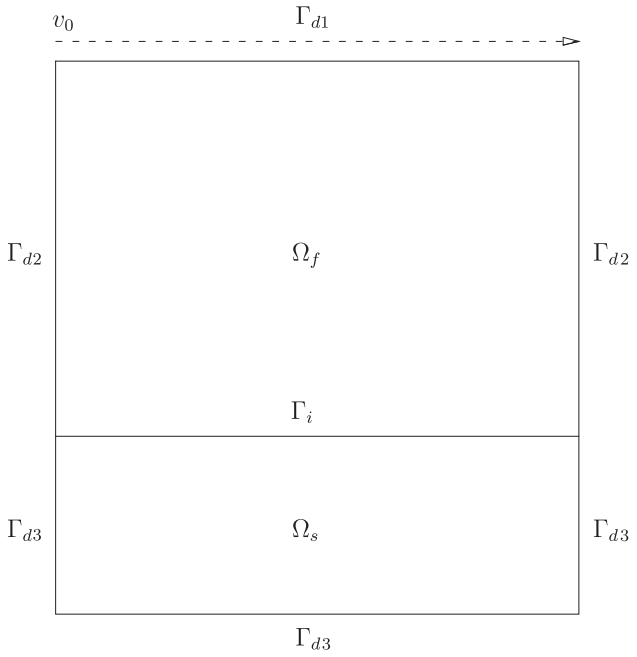

Figure 9. Diagram of 2nd example.

method as a means of sensitivity analysis described by Becker and Rannacher [15, 16]. We set the right-hand side to zero.

6.1. Configuration

Except for the top boundary Γ_{d1} we use homogeneous Dirichlet boundary conditions for all velocities and the displacement. To avoid any unnecessary trouble concerning pressure singularities in the top corners the driving velocity is not constant but instead:

$$v_0 = 0.5 \begin{cases} \sin^2(\pi x/0.6), & x \in [0.0, 0.3] \\ 1, & x \in (0.3, 1.7) \\ \sin^2(\pi(x-2.0)/0.6), & x \in [1.7, 2.0] \end{cases}$$

The width and height of the complete domain we set to 2, the elastic volume at the bottom has a height of 0.5. The material constants are: $\rho_f = \rho_s = 1,\ \nu_f = 0.2,\ \mu_s = 2.0$.

To reach the stationary state we use a pseudo-time-stepping method. We consider a stationary state reached once the kinetic energy of the structure is below a desired tolerance, here: $\|v_s\|^2 \leqslant$ 1e-8. In Figure 10 we display the development of $\|v_s\|^2$ during the pseudo-time-stepping method in regards to the number of degrees of freedom (dof) in the mesh. As expected the kinetic energy goes to zero. The multiple 'bumps' that are seen, occur due to way

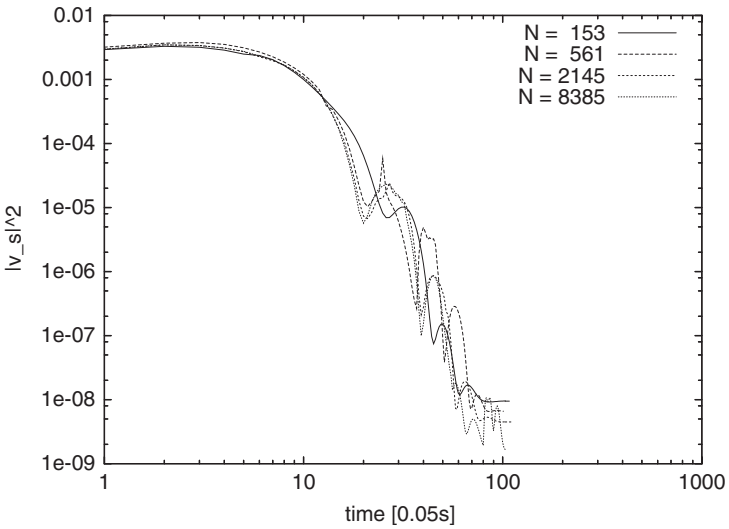

Figure 10. $\|v_s\|^2$ for different 'dof's.

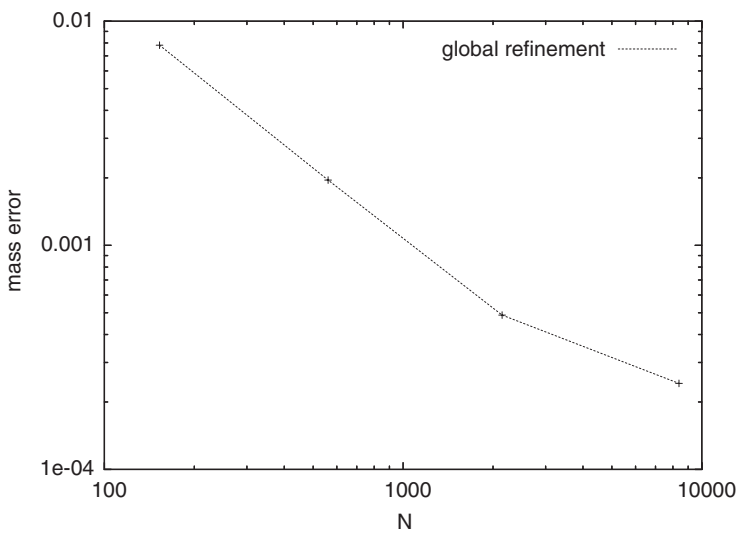

Figure 11. Relative mass error of stationary results.

the elastic structure arrives at its stationary state, by 'swinging' back and forth a few times. At the extreme of each swing, the kinetic energy is at a local minimum.

In Figure 11 we display the mass error of the structure from the final stationary solutions. These values are plotted against the number of degrees of freedom. The results imply that

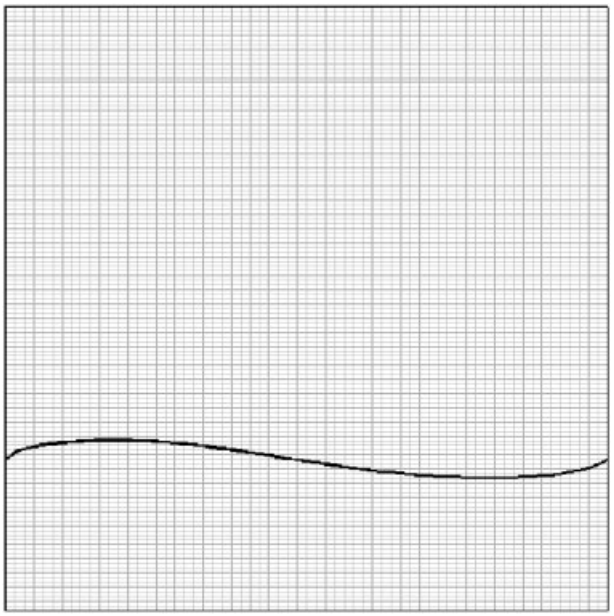

Figure 12. Final position of interface.

that mass error is of the order $O(h^2)$. In Figures 12 and 13 we display the final stationary solution for a globally refined mesh with 8385 degrees of freedom.

Based on the stationary state with the determined domains we develop the dual auxiliary problem. This is the basis of the method used for the *Dual Weighted Residual* method. To shorten the formulation of the auxiliary dual problem we omit higher order terms, e.g. in the Cauchy stress tensor for the structure. Since there is no movement in the structure domain, the mass conservation condition $\operatorname{div} v_u = 0$ is not practical for the sensitivity analysis. For this reason the conservation condition in the structure domain will be $\det(I - \nabla u) - 1 = 0$ from which we omit the higher order terms: $\det(I - \nabla u) - 1 \approx \operatorname{div} u = 0$.

Find $\{v, w, u, p\} \in \{v_D + V\} \times V \times V \times L/\mathbb{R}$, so that

$$
\begin{aligned}
(\partial_t v, \psi) + (\sigma : \varepsilon(\psi)) &= 0 \quad \forall \psi \in V \\
(\chi_f \operatorname{div} v + \chi_s \operatorname{div} u, \psi) &= 0 \quad \forall \psi \in L \\
(\partial_t u - w + w\nabla u, \psi) &= 0 \quad \forall \psi \in L \\
(\chi_s(w - v), \psi) + (\chi_f \nabla w, \nabla \psi) &= 0 \quad \forall \psi \in V
\end{aligned}
$$

With σ and $\chi_{\{s,f\}}$

$$
\begin{aligned}
\sigma &:= \chi_f \sigma_f + \chi_s \sigma_s \\
\sigma_f &:= -pI + v_f(\nabla v + \nabla v^{\mathrm{T}}) \\
\sigma_s &:= -pI + \mu_s(\nabla u + \nabla u^{\mathrm{T}})
\end{aligned}
$$

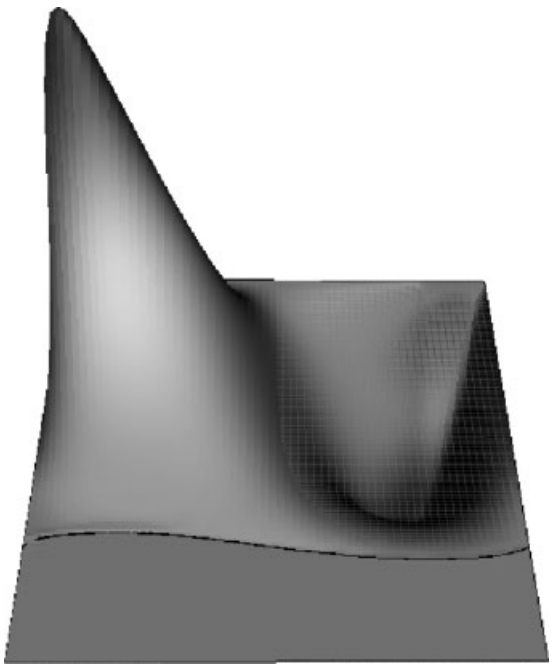

Figure 13. Vertical velocity of final solution.

$$\chi_s = \begin{cases} 1, & x - u \in \widehat{\Omega}_s \\ 0, & \text{otherwise} \end{cases}$$

$$\chi_f = 1 - \chi_s$$

After having reached the stationary state χ_f, χ_s, Ω_f, Ω_s are constant, $w = 0$ and $u_f := \chi_f u$ is known. The model can be written in a reduced form.

Find $U \in U_0 + \widetilde{V}$, so that

$$a(U, \Psi) = 0 \quad \forall \Psi \in \widetilde{V}$$

with

$$a(U, \Psi) := (\sigma(U) : \varepsilon(\Psi_v)) + (\chi_f \operatorname{div} v + \chi_s \operatorname{div} u, \Psi_p)$$

$$+ (\chi_f(u - u_f), \Psi_u) + (\chi_s v, \Psi_u)$$

$$\widetilde{V} := H_0^1(\Omega)^d \times H_0^1(\Omega)^d \times L^2(\Omega)/\mathbb{R}$$

$$U = \{v, u, p\}, \quad \Psi = \{\Psi_v, \Psi_u, \Psi_p\}$$

$$\sigma(U) := \chi_f(-U_p I + 2v_f \varepsilon(U_v)) + \chi_f(-U_p I + 2\mu_s \varepsilon(U_u))$$

Here U_0 is a suitable extension of the prescribed Dirichlet data on the boundaries of Ω.

To derive an *a posteriori* error estimator we first present the basic framework. A more detailed theory is presented in References [15–17]. We have the linear Galerkin forms

$$\begin{aligned} a(U,\Psi) &= F(\Psi) \quad \forall \Psi \in V \\ a(U_h,\Psi_h) &= F(\Psi_h) \quad \forall \Psi_h \in V_h \end{aligned} \tag{10}$$

Using V_h as the test space in the first equation of (10) and subtracting the second equation from this leads to the Galerkin orthogonality

$$a(E,\Psi_h) = 0 \quad \forall \Psi_h \in V_h, \quad (E := U - U_h) \tag{11}$$

For a given linear evaluation functional $J(\cdot)$ the associated dual problem is

$$a(\Psi, Z) = J(\Psi) \quad \forall \Psi \in V \tag{12}$$

By setting $\Psi = E$ and applying the Galerkin orthogonality (11) we obtain

$$\begin{aligned} J(E) = a(E,Z) &= a(E, Z - \Psi_h) \qquad \forall \Psi_h \in V_h \\ &= F(Z - \Psi_h) - a(U_h, Z - \Psi_h) \quad \forall \Psi_h \in V_h \end{aligned}$$

In our case the right-hand side functional F is $(\chi_f u_f, \Psi_u)$. As a first step to approximating the error $J(E)$ we integrate parts of $a(\cdot,\cdot)$ partially on 'cells' in the modified mesh $\widetilde{\mathbb{T}}_h$

$$\widetilde{\mathbb{T}}_h := (\mathbb{T}_h \cap \Omega_f) \cup (\mathbb{T}_h \cap \Omega_s)$$

The mesh $\widetilde{\mathbb{T}}_h$ differs only from $\mathbb{T}_h$ in so far that the cells that contain the fluid–structure interface are subdivided into fluid domain part and structure domain part

$$\begin{aligned} J(E) &= F(Z - \Psi_h) - a(U_h, Z - \Psi_h) \\ &= \sum_{K \in \widetilde{\mathbb{T}}_h} (\operatorname{div} \sigma(U_h), Z_v - \Psi_{h,v})_K - (\tfrac{1}{2}[\sigma(U_h)\cdot n], Z_v - \Psi_{h,v})_{\partial K} \\ &\quad -(\chi_f \operatorname{div} U_{h,v}, Z_p - \Psi_{h,p})_K - (\chi_s \operatorname{div} U_{h,u}, Z_p - \Psi_{h,p})_K \\ &\quad -(\chi_f (U_{h,u} - u_f), Z_u - \Psi_{h,u})_K - (\chi_s U_{h,v}, Z_u - \Psi_{h,u})_K \end{aligned}$$

By applying the triangle inequality to $|J(E)|$ we obtain

$$\begin{aligned} |J(E)| \leqslant \sum_{K \in \widetilde{\mathbb{T}}_h} & \|\operatorname{div} \sigma(U_h)\|_K \|Z_v - \Psi_{h,v}\|_K \\ & + \|\tfrac{1}{2}[\sigma(U_h)\cdot n]\|_{\partial K} \|Z_v - \Psi_{h,v}\|_{\partial K} \\ & + \|\chi_f \operatorname{div} U_{h,v}\|_K \|\chi_f (Z_p - \Psi_{h,p})\|_K \end{aligned}$$

$$
\begin{aligned}
&+ \|\chi_s \operatorname{div} U_{h,u}\|_K \|\chi_s(Z_p - \Psi_{h,p})\|_K \\
&+ \|\chi_f(U_{h,u} - u_f)\|_K \|\chi_f(Z_u - \Psi_{h,u})\|_K \\
&+ \|\chi_s U_{h,v}\|_K \|\chi_s(Z_u - \Psi_{h,u})\|_K
\end{aligned}
$$

We use the interpolation $I_h Z$ of Z for Ψ_h and approximate with Cauchy–Schwarz to

$$
\begin{aligned}
|J(E)| &\leqslant \sum_{K \in \widetilde{\mathbb{T}}_h} \rho_K \omega_K \\
\rho_K^2 &:= \|\operatorname{div} \sigma(U_h)\|_K^2 + h_K^{-1} \|\tfrac{1}{2}[\sigma(U_h)\cdot n]\|_{\partial K}^2 \\
&\quad + \|\chi_f \operatorname{div} U_{h,v}\|_K^2 + \|\chi_s \operatorname{div} U_{h,u}\|_K^2 + \|\chi_s U_{h,v}\|_K^2 \\
\omega_K^2 &:= \|Z_v - I_h Z_v\|_K^2 + h_K \|Z_v - I_h Z_v\|_{\partial K}^2 + \|Z_p - I_h Z_p\|_K^2 + \|Z_u - I_h Z_u\|_K^2
\end{aligned}
\tag{13}
$$

The cell-residuals ρ_K we evaluate directly with the help of post-processing of U_h. The cell-error-weights ω_K we approximate using interpolation estimates

$$
\begin{aligned}
\omega_K^2 &= \|Z_v - I_h Z_v\|_K^2 + h_K \|Z_v - I_h Z_v\|_{\partial K}^2 + \|Z_p - I_h Z_p\|_K^2 + \|Z_u - I_h Z_u\|_K^2 \\
&\leqslant c_I^2 h_K^4 \|\nabla^2 Z_v\|_K^2 + c_I^2 h_K^4 \|\nabla^2 Z_p\|_K^2 + c_I^2 h_K^4 \|\nabla^2 Z_u\|_K^2
\end{aligned}
\tag{14}
$$

The interpolation constant is $c_I \approx 0.1 \ldots 1$. The second derivatives $\nabla^2 Z_{(\cdot)}$ we replace with the discrete second-order difference quotients $\nabla_h^2 Z_{h,(\cdot)}$ that we get from the Ritz projection of Z.

As an example we apply this method for calculating the point-value of the pressure at the point $P = (0.5, 1.0)$. For this we set J to be the approximation of $\int \delta_P p \, \mathrm{d}x$

$$
J(p) = |K_P|^{-1} \int_{K_P} p \, \mathrm{d}x
$$

where K_P is the cell in the Mesh $\mathbb{T}_h$ containing the point P. As a reference value to the pressure at the point P we use the results from a globally refined grid with 33 153 degrees of freedom. The approach we use for the adaptive refinement is straightforward:

1. Calculate primal solution on the mesh starting with the initial state of no deformation.
2. Calculate dual solution of dual problem.
3. With primal and dual solutions determine the cells errors η_K, being the product of the cell-residuals ρ_K and -weights ω_K.
4. Mesh Adaptation: the strategy that we use here is to determine the 30% largest and 10% smallest values of η_K. The largest and smallest values we use to determine which cells to refine and coarsen once. Refinement takes place first. When coarsening, we consider the previous refinement and possible neighbouring cells with hanging nodes. (Refinement and Coarsening, especially concerning hanging nodes, are described in Section 4.) On a 2d mesh with quadrilateral cells this leads to the number of cells approximately doubling with each iteration.
5. If certain criteria have not been met continue with step 1, otherwise go to next step.
6. Post-process and finish.

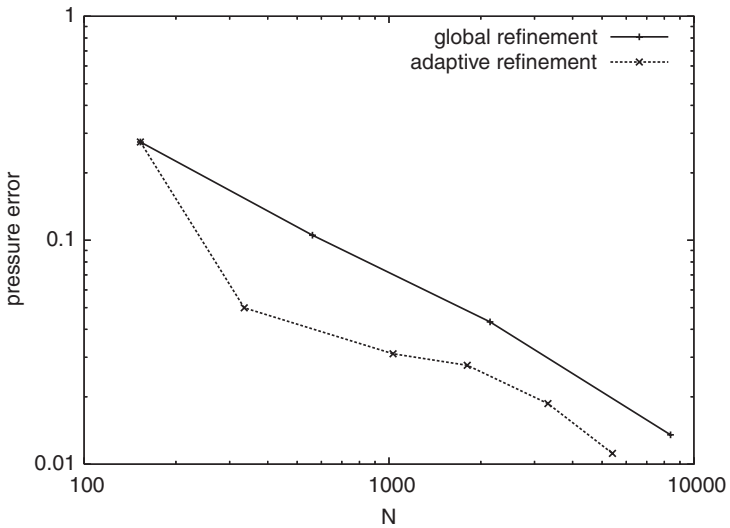

Figure 14. Reduction of the pressure value error.

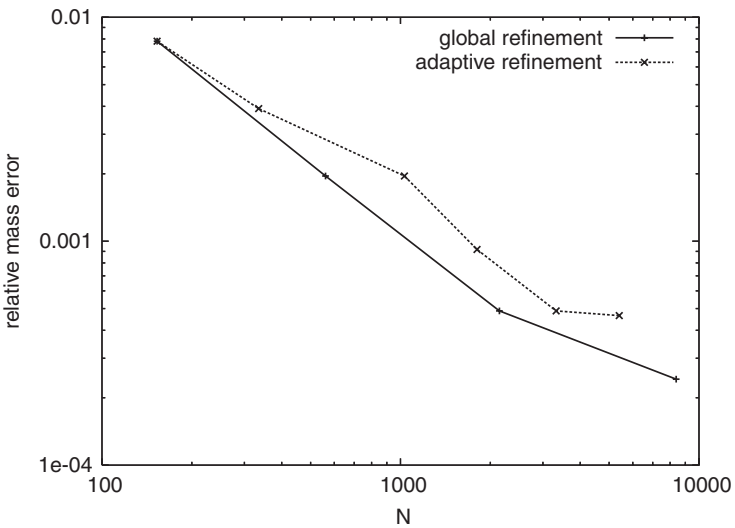

Figure 15. Relative mass error.

In Figures 14–16 we show the results for a few iterations of adaptive refinement. As expected two refinement effects can be observed. There is local refinement around the point of interest and since the position of the fluid–structure interface is a decisive factor for the pressure field, local refinement has also taken place at the interface. Maybe surprising is that in Figure 15

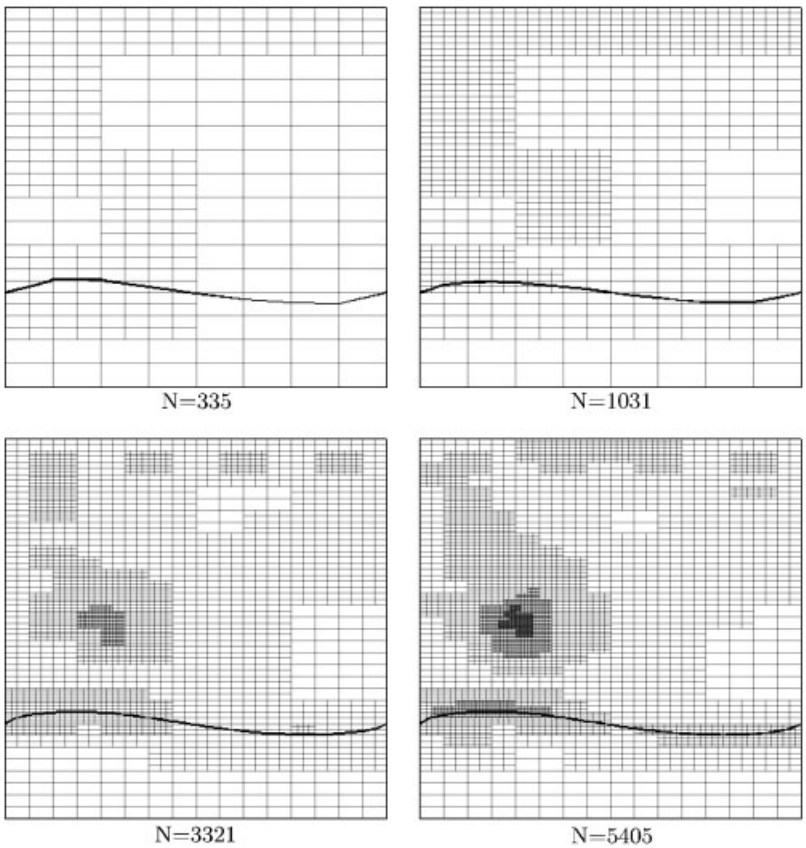

Figure 16. Locally adapted meshes.

there is no reduction of the mass error in the last iteration. This is due to the approach we are using here. After each mesh adaptation cycle a new primal solution is calculated, starting with the initial state of no deformation. The sensitivity analysis though does not take the initial state into account. Mesh adaptation takes place around the final state of the interface, it does not consider its initial state. An easy way of alleviating the mass error problem is to explicitly move a certain amount of local refinements with the interface from one time step to the next. Doing that though in this example would have made it unclear if the local refinement at the final interface position was due to the sensitivity analysis or the explicit movement of interface-bound refinement.

7. SUMMARY AND FUTURE DEVELOPMENT

In this paper we presented a fully variational Eulerian approach for fluid–structure interaction problems. This approach is made possible with the help of the IP set method. The main

advantage of the IP set approach with respect to the level set approach is the improved handling of geometries containing corners. By using the harmonic continuation of data we avoid the occasional need of reinitialization of the IP set. Based on the IP set method numerical simulations of FSI problems with free bodies and large deformations become feasible. This is a main advantage of this method in respect to methods that are based on the ALE approach as described in the introduction.

Results for the Eulerian approach shown in the first example are in good agreement with results obtained based on the ALE approach. To insure a 'fair' comparison of results, both approaches, Eulerian and ALE, were implemented using the otherwise same numerical methods and software library Gascoigne [25].

Results shown in the second example display the conservation of mass to be good, the mass error was of the order $O(h^2)$. Results also showed that the application of the Dual Weighted Residual (DWR) method was feasible and lead to an improvement of convergence of the goal functional.

Based on the fully variational Eulerian approach sensitivity analysis by ways of the DWR method is possible. One direction of future investigation will be to use the DWR method for optimization problems of stationary and instationary FSI problems. Consider for instance in the first example, if we had wanted to change the flag's amplitude and frequency by modifying the material parameters at two material positions. This is an optimization problem that can be addressed with the help of the DWR method.

Also of interest will be to use the DWR to determine to what detail exactly the fluid–structure interaction has to be resolved if one is merely interested in evaluating data that is not immediately connected to the interaction. As a simple example, consider changing the geometry of the driven cavity problem by making fluid cavity ten times higher. If only data at the top is of interest, to what detail is resolving the interaction even necessary? In more complicated (especially instationary) geometries this is a fascinating problem which we plan to address using the DWR method.

REFERENCES

1. Hron J. Fluid–structure interaction with applications in biomechanics. *Ergebnisberichte des Instituts für Angewandte Mathematik*, *Nummer 286*, *FB Mathematik*. University Dortmund: Germany, 2005.
2. Huerta A, Liu WK. Viscous flow with large free-surface motion. *Computer Methods in Applied Mechanics and Engineering* 1988.
3. Wall WA. Fluid–structure interaction with stabilized finite elements. *Ph.D. Dissertation*, *Report No. 31*, Institute of Structural Mechanics, University of Stuttgart, 1999.
4. Tezduyar TE, Behr M, Liou J. A new strategy for finite element flow computations involving moving boundaries and interfaces the deforming-spatial-domain/space-time procedures: I. The concept and preliminary tests. *Computer Methods in Applied Mechanics and Engineering* 1992.
5. Tezduyar TE, Behr M, Liou J. A new strategy for finite element flow computations involving moving boundaries and interfaces—the deforming-spatial-domain/space-time procedures: II. Computation of free-surface ows, two-liquid ows and ows with drifting cylinders. *Computer Methods in Applied Mechanics and Engineering* 1992.
6. Liu C, Walkington NJ. An Eulerian description of fluids containing visco-elastic particles. *Archive for Rational Mechanics and Analysis* 2001; **159**(3):229–252.
7. Joseph DD, Renardy YY. *Fundamentals of Two-fluid Dynamics*, *part I*. Mathematical Theory and Applications. Springer: New York, 1993.
8. Joseph DD, Renardy YY. *Fundamentals of Two-fluid Dynamics*, *part II*. Lubricates transport, drops and miscible liquids. Springer-Verlag: New York, 1993.
9. Hirt CW, Nichols BD. Volume of Fluid (VOF) method for the dynamics of free boundaries. *Journal of Computational Physics* 1981; **39**(1):201–225.
10. Chang YC, Hou TY, Merriman B, Osher S. A level set formulation of Eulerian interface capturing methods for incompressible fluid flows. *Journal of Computational Physics* 1996; **123**:449–464.

11. Osher S, Sethian JA. Propagation of fronts with curvature based speed: algorithms based on Hamilton–Jacobi formulations. *Journal of Computational Physics* 1988; **79**:12.
12. Sethian JA. *Level Set Methods and Fast Marching Methods*. Cambridge University Press: Cambridge, MA, 1999.
13. Legay A, Chessa J, Belytschko T. An Eulerian–Lagrangian method for fluid–structure interaction based on level sets. *Computer Methods in Applied Mechanics and Engineering* 2004, submitted.
14. Becker R, Braack M. A two-level stabilization scheme for the Navier–Stokes equations. *Enumath 2003 Proceedings*. Springer: Berlin, 2003; 123–130.
15. Becker R, Rannacher R. An optimal control approach to error estimation and mesh adaptation in finite element methods. In *Acta Numerica 2000*, Iserles A (ed.). Cambridge University Press: Cambridge, MA, 2001; 1–101.
16. Becker R, Rannacher R. A feed-back approach to error control in finite element methods: basic analysis and examples. *East-West Journal of Numerical Mathematics* 1996; **4**:237–264.
17. Bangerth W, Rannacher R. *Adaptive Finite Element Methods for Differential Equations*. Birkhaüser, 2003.
18. Carey G, Oden J. *Finite Elements*, *Computational Aspects*, vol. III. Prentice-Hall: Englewood Cliffs, NJ, 1984.
19. Ciarlet P. *Finite Element Methods for Elliptic Problems*. North-Holland: Amsterdam, 1978.
20. Johnson C. *Numerical Solution of Partial Differential Equations by the Finite Element Method*. Cambridge University Press: Cambridge, U.K., 1987.
21. Bristeau MO, Glowinski R, Periaux J. Numerical methods for the Navier–Stokes equations. *Computer Physics Reports* 1987; **6**:73–187.
22. Kloucek P, Rys FS. Stability of the fractional step θ-scheme for the nonstationary Navier–Stokes equations. *SIAM Journal on Numerical Analysis* 1994; **34**:1312–1335.
23. Müller-Urbaniak S. Eine Analyse des Zwischenschritt-θ-Verfahrens zur Lösung der instationären Navier–Stokes-Gleichungen. *SFB 359 Preprint*. *No. 94-01*, IWR, Universität Heidelberg, 1994.
24. Saramito P. A new θ-scheme algorithm and incompressible FEM for viscoelastic fluid flows. *Mathematical Modelling and Numerical Analysis* 1994; **28**:1–34.
25. Gascoigne. A C++ numerics library for scientific computing. http://gascoigne.uni-hd.de/
26. Turek S, Schäfer M. Benchmark computations of laminar flow around a cylinder. In *Flow Simulation with High-Performance Computers II*, Hirschel EH, Durst F, Krause E, Rannacher R (eds), Notes on numerical fluid mechanics, vol. 52. Vieweg: Braunschweig, 1996.
27. Becker R, Braack M. A finite element pressure gradient stabilization for the Stokes equations based on local projections. *Calcolo* 2001; **38**(4):173–199.
28. Suttmeier F-T. An adaptive displacement/pressure finite element scheme for treating incompressibility effects in elasto-plastic materials. *Numerical Methods for Partial Differential Equations* 2001; **17**:369–382.
29. VisuSimple. An open source interactive visualization utility for scientific computing, http://visusimple.uni-hd.de/

